Dyes and Pigments 94 (2012) 393–402

Contents lists available at SciVerse ScienceDirect

Dyes and Pigments

journal homepage: www.elsevier.com/locate/dyepig

Water soluble squaraine dyes for use as colorimetric stains in gel electrophoresis

Daniel E. Lynch*, Andrew N. Kirkham, Mohammed Z.H. Chowdhury, Elizabeth S. Wane, John Heptinstall

Faculty of Health and Life Sciences, Coventry University, Coventry CV1 5FB, UK

ARTICLE INFO

Article history:
Received 3 November 2011
Received in revised form
26 January 2012
Accepted 2 February 2012
Available online 20 February 2012

Keywords:
Squaraine dyes
X-ray crystal structure
Gel electrophoresis
Protein detection
Colorimetric stain
Fluorescence

ABSTRACT

Here we report that the difficulties encountered in the synthesis of a dual-pendant sulfonate bis(indolenine)squaraine dye can be overcome through the use of equimolar amounts of the common reaction catalyst, thus creating an organic salt between the sulfonate groups and the protonated catalyst. Thus, a range of water-soluble dyes can further be prepared, by simply altering the catalyst. Crystal structures of four subsequent derivatives, prepared in this manner, are reported and show that, although the squaraine moieties remain essentially planar, the packing lattices can vary significantly, and the expectation that both sulfonic acid groups will protonate a stoichiometric amount of the available organic base catalyst is also demonstrated by one structure to not be fully true. Two of the dyes, whose crystal structures are reported, proved to be suitable as colorimetric stains for protein separation in sodium dodecylsulphate polyacrylamide gel electrophoresis (SDS-PAGE), and an optimal method for staining is reported. Results obtained for a fifth dye, crystal structure not obtained, are also reported. In all cases the results were compared against non-colloidal Coomassie Brilliant Blue (CBB) and it was found that the limit of detection for all squaraine derivatives examined were comparable with that of CBB although the resolution between protein bands was better. In addition, it was discovered that gels stained with the fifth dye (presented in this study) could be imaged in UV excitation/fluorescent imaging mode. The image robustness (or colour fastness) of all squaraines was found to be good for only a few hours.

1. Introduction

Bis(indolenine)squaraines have been significant in the development of squaraine chemistry [1–3], from both a spectroscopic perspective [4–11] and a structural one [12–18]. They were one of the first types of squaraine dyes for which a non-symmetrical synthetic route was developed [19,20] and they have been instrumental in the development of squaraine dyes as biological markers [19,21–28]. This is not only due to the fact that their fluorescence increases ten-fold upon interaction with proteins but also because they can be substituted with sulfonate groups, thus rendering the otherwise water insoluble squaraine dye as water soluble [21,22,24–28]. Sulfonate groups can be attached at either the 5-position on the indolenine ring or as pendant alkyl-sulfonates from the indolenine nitrogen atom. The significance of their non-symmetrical synthesis is that only one pendant *N*-hydroxy succinimide group can be attached, thus creating a biomarker where only one point of attachment (to a biological species) is available. A multitude of dyes of this type have been presented in both the scientific journal [21,22,24–28] and patent [29–33] literatures. However, one area where the use of bis(indolenine)squaraine dyes has been relatively ignored is as a colorimetric stain for protein separation in sodium dodecylsulphate polyacrylamide gel electrophoresis. The reason for this may stem from the overt success of the most commonly used commercial dye for this application; Coomassie Brilliant Blue [34]. To date, only one chromophore based on a squaraine structure has been reported as a stain for sodium dodecylsulphate polyacrylamide gel electrophoresis [35]. In this present study we set out to synthesize a simple, water soluble bis(indolenine)squaraine derivative and evaluate its performance as a protein stain in sodium dodecylsulphate polyacrylamide gel electrophoresis. As part of this study a beneficial modification to the synthesis (Fig. 1) was discovered that yielded a number of new squaraine derivatives. Reported here is the synthesis, crystal structures and solution spectroscopic properties of four new water soluble bis(indolenine)squaraine derivatives as well as their performance as colorimetric stains for protein separation in sodium dodecylsulphate polyacrylamide gel electrophoresis. The stain performance of a fifth squaraine derivative, whose crystal structure was not determined, is also reported.

* Corresponding author. Current address: Exilica Limited, The Technocentre, Puma Way, Coventry CV1 2TT, UK. Tel.: +44 (0) 24 7688 8505.
E-mail address: d.lynch@exilica.co.uk (D.E. Lynch).

0143-7208/$ – see front matter © 2012 Elsevier Ltd. All rights reserved.
doi:10.1016/j.dyepig.2012.02.001

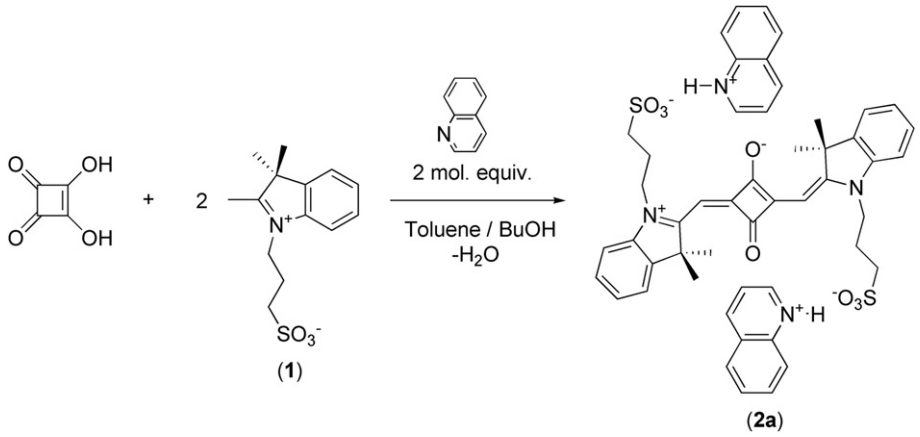

Fig. 1. Schematic showing the synthetic route developed in this study.

2. Materials and methods

2.1. Synthesis

All chemicals were purchased from Sigma–Aldrich and were used as received without further purification. The water used in this study was purified using reverse osmosis techniques. Infrared spectra were recorded as KBr discs using a Nicolet 205 FT-IR spectrometer. Electrospray mass spectra were recorded in both positive (ES^+) and negative (ES^-) ion mode on a Micromass Platform mass spectrometer. ^1H NMR spectrum for **2a** was recorded on a Bruker Avance 300 MHz instrument whereas the remaining spectra were recorded on a Bruker Avance 400 MHz instrument, all in deuterated dimethyl sulphoxide (DMSO-d_6). C,H,N analysis was measured using a Thermo FlashEA 1112 Elemental Analyser.

2.1.1. 2,3,3-Trimethyl-1-(propan-3-sulfonyl)indolenine (*1*)

2,3,3-Trimethylindolenine (3.00 g, 18.8 mmol) was heated under reflux with an equimolar amount of 1,3-propanesultone (2.30 g, 18.8 mmol) in toluene (100 mL) for 24 h, with constant stirring. Upon cooling, the product was separated by filtration, dried and washed with petroleum ether (40/60). The product was collected as a dry red powder and was used without further purification. Yield: 5.18 g (98%).

2.1.2. Bis-quinolinium 2,4-bis-(3,3-dimethyl-(1-propan-3-sulphonate)-2-indolinylidenemethyl)cyclobutene-1,3-diolate (*2a*)

Squaric acid (200 mg, 1.75 mmol) was added to 2.0 M equivalents of 2,3,3-trimethyl-1-(propan-3-sulphonyl)-indolenine **1** (0.98 g, 3.5 mmol) and quinoline (0.45 g, 3.5 mmol) in a 1:1 v/v mix of 1-butanol:toluene (30 mL) and the mixture was then heated under reflux for 16 h using a Dean and Stark apparatus. Upon cooling, metallic green crystals were collected *in vaccuo*, washed with petroleum ether (60/40), and were used without further purification. Yield: 1.05 g (67%). UV/Vis (H_2O) λ_{max} (log ε): 624 (5.41). IR (KBr) ν_{max}: 1580 (C–O). ^1H NMR (300.13 MHz, DMSO-d_6) δ: 1.65 (12H, s, CH_3), 2.05 (4H, quintet, $J = 6.7$, CH_2), 2.60 (4H, t, $J = 6.7$, $CH_2SO_3^-$), 4.20 (4H, m, NCH_2), 5.70 (2H, s, CH=), 7.15 (2H, t, $J = 7.7$, ArH), 7.33 (2H, t, $J = 7.7$, ArH), 7.44 (2H, d, $J = 7.9$, ArH), 7.51 (2H, d, $J = 6.$, ArH), 7.92 (2H, td, $J = 6.7$, $J = 1.1$, ArH), 8.04 (2H, d, $J = 8.4$, ArH), 8.06 (2H, d, $J = 8.4$, ArH), 8.11 (2H, td, $J = 6.8$, $J = 1.2$, ArH), 8.24 (2H, d, $J = 8.5$, ArH), 8.34 (2H, d, $J = 7.9$, ArH), 9.11 (2H, d, $J = 8.1$, ArH), 9.30 (2H, dd, $J = 4.8$, $J = 1.5$, ArH). ES^+: 130.1 ($C_9H_8N^+$; calc. 130.2). ES^-: 319.3 ($C_{32}H_{34}N_2O_8S_2^{2-}$; calc. 638.8).

2.1.3. 5-Nitroquinolinium) 2-(3,3-dimethyl-(1-propan-3-sulphonate)-2-indolinylidenemethyl)-4-(3,3-dimethyl-(1-propan-3-sulfonic acid)-2-indolinylidenemethyl) cyclobutene-1,3-diolate (*2b*)

Squaric acid (100 mg, 0.88 mmol) was added to 2.0 M equivalents of 2,3,3-trimethyl-1-(propan-3-sulphonyl)-indolenine **1** (495 mg, 1.76 mmol) and 5-nitroquinoline (307 mg, 1.76 mmol) in a 1:1 v/v mix of 1-butanol:toluene (30 mL) and the mixture was then refluxed for 16 h using a Dean and Stark apparatus. Upon cooling, blue/purple crystals were collected *in vaccuo*, washed with petroleum ether (60/40), and were used without further purification. Yield: 377 mg (51%). UV/Vis (H_2O) λ_{max} (log ε): 624 (5.48). IR (KBr) ν_{max}: 1600 (C–O). ^1H NMR (400.13 MHz, DMSO-d_6) δ: 1.70 (12H, s, CH_3), 2.05 (4H, quintet, $J = 6.8$, CH_2), 2.58 (4H, t, $J = 6.8$, $CH_2SO_3^-$), 4.25 (4H, m, NCH_2), 5.85 (2H, s, CH=), 6.50 (bs, $H_2O/SO_3H/N^+H$), 7.18 (2H, t, $J = 7.6$, ArH), 7.35 (2H, t, $J = 7.6$, ArH), 7.45 (2H, d, $J = 7.2$, ArH), 7.52 (2H, d, $J = 7.2$, ArH), 7.83 (½H, d, $J = 8.7$, ArH), 7.84 (½H, d, $J = 8.7$, ArH), 7.97 (½H, d, $J = 7.5$, ArH), 7.99 (½H, d, $J = 7.5$, ArH), 8.46 (2H, t, $J = 8.4$, ArH), 8.87 (1H, d, $J = 9.0$, ArH), 9.10 (1H, dd, $J = 5.3$, $J = 1.6$, ArH). ES^-: 319.3 ($C_{32}H_{34}N_2O_8S_2^{2-}$; calc. 638.8).

2.1.4. Bis-(8-hydroxyquinolinium) 2,4-bis-(3,3-dimethyl-(1-propan-3-sulphonate)-2-indolinylidenemethyl)cyclobutene-1,3-diolate (*2c*)

Same procedure as for **2b** except: 8-hydroxyquinoline (255 mg, 1.76 mmol). Upon cooling, metallic green crystals were collected *in vaccuo*, washed with petroleum ether (60/40), and were used without further purification. Yield: 565 mg (65%). UV/Vis (H_2O) λ_{max} (log ε): 624 (5.45). IR (KBr) ν_{max}: 1595 (C–O). ^1H NMR (400.13 MHz, DMSO-d_6) δ: 1.70 (12H, s, CH_3), 2.05 (4H, m, CH_2), 2.60 (4H, m, $CH_2SO_3^-$), 4.00–5.00 (bs, H_2O), 5.90 (2H, bs, CH=), 7.00–7.80 (14H, bm, ArH/N^+H), 7.89 (2H, d, $J = 8.1$, ArH), 7.91 (2H, d, $J = 8.1$, ArH), 8.88 (2H, d, $J = 7.5$, ArH), 9.10 (2H, dd, $J = 3.8$, $J = 1.2$, ArH). ES^+: 146.2 ($C_9H_8NO^+$; calc. 146.2). ES^-: 319.5 ($C_{32}H_{34}N_2O_8S_2^{2-}$; calc. 638.8).

2.1.5. Bis-acridinium 2,4-bis-(3,3-dimethyl-(1-propan-3-sulphonate)-2-indolinylidenemethyl)cyclobutene-1,3-diolate (*2d*)

Same procedure as for **2b** except: acridine (315 mg, 1.76 mmol). Upon cooling, metallic green crystals were collected *in vaccuo*, washed with petroleum ether (60/40), and were used without further purification. Yield: 600 mg (66%). UV/Vis (H_2O) λ_{max} (log ε): 624 (5.17). IR (KBr) ν_{max}: 1580 (C–O). ^1H NMR (400.13 MHz, DMSO-d_6) δ: 1.67 (12H, s, CH_3), 2.05 (4H, quintet, $J = 7.0$, CH_2), 2.62 (4H, t, $J = 8.4$, $CH_2SO_3^-$), 4.25 (4H, m, NCH_2), 5.82 (2H, s, CH=), 7.16 (2H, t, $J = 6.3$, ArH), 7.23 (2H, d, $J = 6.7$, ArH), 7.32 (2H, t, $J = 6.3$, ArH), 7.43 (2H, bs, N^+H), 7.49 (2H, d, $J = 6.7$, ArH), 7.88 (4H, t, $J = 6.7$, ArH), 8.22

(4H, t, $J = 6.0$, ArH), 8.33 (4H, d, $J = 7.0$, ArH), 8.46 (4H, d, $J = 7.0$, ArH), 9.85 (2H, s, ArH). ES^+: 180.2 ($C_{13}H_{10}N^+$; calc. 180.2). ES^-: 319.5 ($C_{32}H_{34}N_2O_8S_2^{2-}$; calc. 638.8).

2.1.6. Bis-piperidinium 2,4-bis-(3,3-dimethyl-(1-propan-3-sulphonate)-2-indolinylidenemethyl)cyclobutene-1,3-diolate (**2e**)

Same procedure as for **2b** except: piperidinium (150 mg, 1.76 mmol). Upon cooling, a metallic green powder was collected *in vaccuo*, washed with petroleum ether (60/40), and used without further purification. Yield: 250 mg (35%). UV/Vis (H_2O) λ_{max} (log ε): 624 (5.43). IR (KBr) ν_{max}: 1580 (C—O). ^1H NMR (400.13 MHz, DMSO-d_6) δ: 1.61 (4H, m, CH_2), 1.71 (8H, quintet, $J = 5.7$, CH_2), 1.72 (12H, s, CH_3), 2.09 (4H, quintet, $J = 7.3$, CH_2), 2.61 (4H, t, $J = 7.0$, $CH_2SO_3^-$), 3.05 (8H, t, $J = 5.8$, NCH_2), 4.27 (4H, t, $J = 7.6$, NCH_2), 5.85 (2H, s, CH═), 7.15 (2H, t, $J = 7.5$, ArH), 7.33 (2H, td, $J = 7.6$, $J = 1.2$, ArH), 7.42 (2H, d, $J = 8.0$, ArH), 7.45 (2H, d, $J = 7.5$, ArH), 8.22 (4H, bs, N^+H). ES^-: 319.4 ($C_{32}H_{34}N_2O_8S_2^{2-}$; calc. 638.8).

2.1.7. X-ray crystallographic analysis

Single crystals of the four squaraine dyes **2a**—**2d** were obtained in each case by the slow evaporation of a dilute solution of each dye in chloroform. Crystallographic data, for **1**, was collected on an Enraf—Nonius CAD-4 using monochromatized Mo-Kα X-ray radiation ($\lambda = 0.71073$ Å), for **2c**, was collected on a Bruker Nonius Kappa CCD area diffractometer using monochromatized Mo-Kα X-ray radiation ($\lambda = 0.71073$ Å) equipped with an Oxford Cryosystem low temperature device, and for **2a**, **2b**, and **2d**, was collected on a Bruker SMART APEX2 CCD diffractometer using synchrotron radiation ($\lambda = 0.6848$ Å). All structures were solved by direct methods SHELX97, and refined by full-matrix least-squares calculations. Crystal data for **1**: $C_{14}H_{23}NO_5S$, $Mw = 317.39$, monoclinic, $P2_1/c$, $Z = 4$, $a = 10.767(4)$, $b = 12.782(2)$, $c = 11.891(6)$ Å, $\beta = 103.88(2)^\circ$, $D_{calcd} = 1.327$ g cm^{-3}, $T = 298(2)$ K, $F(000) = 680$, $\mu = 0.224$ mm^{-1}, 2923 reflections were collected, 2772 unique ($R_{int} = 0.2284$), 845 observed ($F > 4\sigma(F)$), 202 parameters, $R_1 = 0.0788$, $wR_2 = 0.1920$. Crystal data for **2a**: $C_{50}H_{50}N_4O_8S_2$, $Mw = 899.08$, monoclinic, $P2_1/c$, $Z = 2$, $a = 13.3034(9)$, $b = 6.3940(4)$, $c = 27.4465(16)$ Å, $\beta = 110.965(3)^\circ$, $D_{calcd} = 1.370$ g cm^{-3}, $T = 120(2)$ K, $F(000) = 948$, $\mu = 0.184$ mm^{-1}, 13,214 reflections were collected, 3820 unique ($R_{int} = 0.0579$), 2655 observed ($I > 2\sigma(I)$), 291 parameters, $R_1 = 0.0452$, $wR_2 = 0.1023$. Crystal data for **2b**: $C_{82}H_{92}N_8O_{24}S_4$, $Mw = 1701.92$, monoclinic, $C2/c$, $Z = 4$, $a = 44.255(2)$, $b = 6.6710(4)$, $c = 26.8252(14)$ Å, $\beta = 90.732(2)^\circ$, $D_{calcd} = 1.428$ g cm^{-3}, $T = 120(2)$ K, $F(000) = 3584$, $\mu = 0.205$ mm^{-1}, 26,967 reflections were collected, 6882 unique ($R_{int} = 0.0483$), 5121 observed ($I > 2\sigma(I)$), 639 parameters, $R_1 = 0.0743$, $wR_2 = 0.1855$. Crystal data for **2c**: $C_{50}H_{56}N_4O_{13}S_2$, $Mw = 985.11$, triclinic, $P\bar{1}$, $Z = 2$, $a = 11.5003(12)$, $b = 14.1179(12)$, $c = 14.8336(15)$ Å, $\alpha = 96.743(6)$, $\beta = 98.322(4)$, $\gamma = 91.954(6)^\circ$, $D_{calcd} = 1.384$ g cm^{-3}, $T = 120(2)$ K, $F(000) = 1040$, $\mu = 0.184$ mm^{-1}, 44,316 reflections were collected, 9235 unique ($R_{int} = 0.1053$), 5504 observed ($I > 2\sigma(I)$), 656 parameters, $R_1 = 0.0961$, $wR_2 = 0.1594$. Crystal data for **2d**: $C_{58}H_{58}N_4O_{10}S_2$, $Mw = 1035.22$, triclinic, $P\bar{1}$, $Z = 1$, $a = 6.710(2)$, $b = 9.413(4)$, $c = 19.966(7)$ Å, $\alpha = 91.061(4)$, $\beta = 93.003(4)$, $\gamma = 102.736(4)^\circ$, $D_{calcd} = 1.400$ g cm^{-3}, $T = 120(2)$ K, $F(000) = 546$, $\mu = 0.177$ mm^{-1}, 12,308 reflections were collected, 6720 unique ($R_{int} = 0.0328$), 5294 observed ($I > 2\sigma(I)$), 342 parameters, $R_1 = 0.1477$, $wR_2 = 0.4343$. Crystallographic data (**1** (CCDC 798555), **2a** (CCDC 798554), **2b** (CCDC 798556), **2c** (CCDC 798557), **2d** (CCDC 798558)) have been deposited at the CCDC, 12 Union Road, Cambridge CB2 1EZ, UK.

2.2. Materials

Bovine serum albumin (BSA), bromophenol blue, Coomassie Brilliant Blue R-250 (CBB), 2,2′,2″,2‴-(ethane-1,2-diyldinitrilo) tetraacetic acid (EDTA), glacial acetic acid, glycerol, hydrochloric acid (HCl), human serum albumin (HSA), mercaptoethanol, methanol, polyethyleneglycol (PEG), sodium acetate, sodium dodecylsulfate (SDS), sucrose, 1,2-bis(dimethylamino)ethane (TEMED), and 2-amino-2-hydroxymethylpropane-1,3-diol (Tris) were purchased from Sigma—Aldrich and were used as received without further purification. 40% Acrylamide solution, 1 M Tris—HCl buffer solutions (pH 8.5 and pH 6.0), 20% SDS solution, 10% ammonium persulfate (APS) solution, and a premixed 10× Tris—glycine—SDS Laemmli running buffer were all supplied by Scie-Plas and stored at 4 °C when not in use.

ProteMix Protein Standard containing 12 protein fractions[1] (including two insulin fractions) with a molecular weight ranging from 220 kDa (Myosin from *Oryctol. cuniculus* muscle tissue) to 3.4 and 2.5 kDa (Insulin from *Bos taurus* pancreatic tissue) was purchased from Anamed and was stored at −18 °C before being warmed to room temperature for use, as it was pre-prepared in its own sample buffer. A 'homemade' protein ladder solution was prepared using HSA (80 kDa), BSA (66 kDa), bovine carbonic anhydrase (29 kDa) and insulin (3.4 and 2.5 kDa; from bovine pancreas) in water at twice the desired concentrations (400 μg/mL) before preparation in sample buffer. Relative protein concentrations were determined individually using Lowry assays [36], and a correction factor applied to equalize the protein concentrations in the final solution. Rat liver mitochondrial supernatants were sourced at Coventry University and prepared by lysis followed by centrifugal separation in 0.25 M sucrose/20% PEG, and were then dialysed to remove the salt content, before preparing in sample buffer. Dialysis of the rat liver sample was performed in sections of dialysis tubing (8/32″), cut to a length of 10 cm and soaked in 250 mL water with 0.25 g EDTA for 16 h. These tubes were then capped at one end with a plastic clip and 2 mL of rat liver supernatant pipetted into them. The other end was then clipped and the tubes placed in 2 L of stirred water, for 24 h at 4 °C with the water being changed twice at regular intervals. The total protein concentration of the lysed mitochondrial supernatants was then determined using the Lowry assay, using BSA as a standard. The sample buffer used to prepare all protein samples, except the ProteMix standard, was made by adding 2.5 mL 0.488 M Tris—acetate buffer (pH 8.0), 0.25 g of SDS, 2 mL (1.46 g) glycerol, 0.05 mL mercaptoethanol, and 0.5 mL of 0.5% bromophenol blue solution in a 10 mL volumetric flask, and then diluting to the mark with water. All samples and standards were prepared for electrophoretic separation by vortex mixing in 1:1 proportions with the sample buffer followed by heating to at least 95 °C for 3 min (water bath).

2.3. Spectroscopic measurements

Visible absorption spectra were recording on a Shimadzu UV-1650 UV/visible spectrometer. Molar absorptivity for each dye derivative was determined by serial dilution from 1×10^{-5} M standard solutions, using ten results for each calculation.

2.4. Gel casting procedure

The gels used in the sodium dodecylsulphate polyacrylamide gel electrophoresis (SDS-PAGE) experiments were made using

[1] Molecular weight fractions (kDa): 220 (Myosin from *Oryctol. cuniculus* muscle tissue), 116 (β-Galactosidase from *E. coli*), 97.0 (Glycogen-Phosphorylase from *Oryctol. cuniculus* muscle tissue), 66.0 (Albumin from *Bos taurus* serum), 55.6 (Glutamate Dehydrogenase from *Bos taurus* liver), 36.5 (Lactate Dehydrogenase from *Sus scrofa* muscle tissue), 29.0 (Carbonic Anhydrase from *Bos taurus* erythrocytes), 20.0 (Trypsin inhibitor from *Glycine max*), 14.0 (Lysozyme from *Gallus gallus* egg white), 6.1 (Aprotinin from *Bos Taurus* lung tissue), and 3.4 and 2.5 (Insulin from *Bos taurus* pancreatic tissue).

a Laemmli type SDS-PAGE method [34], with a 10% resolving gel and a 4% stacking gel. All of the gels were cast using Scie-Plas mini-gel casting apparatus. All glass plates were cleaned by soaking in 0.1 M HCl solution, followed by a water rinse, a second wash in a diluted Decon cleaning solution, and a further water rinse with a final wash in 85% ethanol solution before being left to air dry, prior to being loaded into the casting cassettes. Four gels could be cast from the following formulation: 11.0 mL water, 7.5 mL of 40% acrylamide solution, 11.25 mL of 1 M Tris–HCl buffer solution (pH 8.5), 150 μL of 20% SDS solution, 150 μL of 10% APS solution, and 30 μL of TEMED. Solutions were thoroughly mixed in a beaker with a glass rod immediately prior to casting, which incorporated pipetting the mixed solution between the glass plates. Gels were left to set for 30–45 min. 3 mm of space was left below the level that the comb occupied at the top of the cassette to allow room for the stacking gel. The gel was then overlaid with 200 μL of water saturated with *t*-butanol to ensure a flat upper surface. After the resolving gel set the water/*t*-butanol solution was rinsed off with water, and any remaining water removed using the corner of a filter paper. The stacking gel was prepared by the mixing of the following solutions: 1.15 mL 40% acrylamide solution, 1.25 mL Tris–HCl buffer solution (pH 6.0), 7.5 mL water, 50 μL of 20% SDS solution, 40 μL of 10% APS solution, and 7.5 μL of TEMED. Stacking gel solutions were thoroughly mixed in a beaker with a glass rod and were then pipetted between the glass plates until the stacking gel solution was 2–5 mm from the top of the cassette. A 10-well comb was then inserted into the top of the stacking gel and the mixture left to set for 60 min. The combs were then removed and the gels used that day.

2.5. Gel running procedure

Electrophoretic separations were run using a Consort E844 power pack, and Scie-Plas tanks, gel cassettes and glass gel plates. The power pack was set at 200 V (constant), 400 mA (maximum), with a separation time of 1 h. The Scie-Plas running buffer was diluted with water prior to use, as directed in the running buffer instructions, and consisted of 0.25 M Tris, 1.92 M glycine, and 1% SDS with a stated pH value of 8.6. The buffer solution was used to fill the tanks to capacity to help dissipate build up of heat during the electrophoretic separations. Protein samples and standards were carefully pipetted into the gel sample wells, immediately prior to the start of the electrophoretic separation. For each gel, lanes 1 and 10 were loaded with the ProteMix protein standard, and lanes 2–9 were either loaded with a two-fold homemade protein ladder (HSA (80 kDa), BSA (66 kDa), carbonic anhydrase (29 kDa) and insulin (3.4 and 2.5 kDa)) serial dilution of 200 μg/mL serial albumin, giving a concentration range of 200–1.6 μg/mL or 100–0.8 ng (spurious accuracy) of protein per band or a two-fold serial dilution of lysed mitochondrial supernatant starting from 12 μg of total protein.

2.6. Coomassie brilliant blue R-250 staining procedure

Upon completion of the electrophoretic separation, gels were removed from the glass plates and rinsed in water before being washed in 25 mL of fixing solution (10% methanol, 10% acetic acid), for at least 30 min. In each case the fixing solution was poured off the gel (no rinsing). 25 mL CBB stain solution, containing 0.15 g Coomassie Brilliant Blue R-250, 60 mL methanol, 15 mL glacial acetic acid, and 75 mL water was then poured into a sealable plastic staining vessel containing the gel, and placed on a shaker for between 1 h and 16 h. Following staining, the solution was poured off (which was filtered and reused 4–5 times), and the residual dye solution was rinsed off both the gel and staining vessel using water. Gels were destained in 25 mL of an aqueous solution containing 10% methanol and 10% acetic acid solution, called the CBB destain solution. This solution was changed, and replaced by fresh solution, when the dye concentration reached a visible colorimetric equilibrium with the gel. Destaining continued until suitably low background coloration was achieved. All steps were undertaken at room temperature and involved the use of a mechanical shaker.

2.7. Colorimetric staining with squaraine dyes

Staining with all squaraine dye derivatives was undertaken using 25 mL aqueous solutions with a dye concentration of 1×10^{-3} M (unless otherwise stated). Gels were removed from the glass plates immediately upon completion of the electrophoretic run and were rinsed in water, before being placed in a sealable plastic staining vessel. Gels were fixed in 25 mL of an aqueous solution containing 10% methanol and 10% acetic acid for a minimum of 20 min. The fixing solutions were poured from the staining vessel, and the gels rinsed twice for 10 min in 25 mL of water to remove the acid and/or methanol before the gels were stained. The stain solution was then placed in the staining vessel with the gels, and staining was allowed to proceed for between 1 h and 16 h. Stain solution was poured away and gels were rinsed in water to remove the excess dye from the gel and the staining vessel. Gels were destained using the minimum amount of the CBB destain solution (an aqueous solution containing 10% methanol and 10% acetic acid) required to completely submerge the gels. Destain solution was replaced once the concentration of dye had reached a level that appeared to be similar to that of the gel background. The destaining process was repeated until the gel backgrounds appeared to be suitably clear upon visual examination. All steps were undertaken at room temperature and involved the use of a mechanical shaker.

2.8. Gel imaging

All gels were imaged, immediately following destaining, using a Bio-Rad gel documentation system, with a white light epi-illuminator and a white background.

3. Results and discussion

3.1. Synthesis

The literature method for the preparation of **1** states that it can be prepared by heating equimolar amounts of 2,3,3-trimethylindolenine and propane sultone, without any solvent [37]. This is possible because both chemicals, at room temperature, are liquids that are miscible in each other. Upon heating, the product remains a liquid until the mixture is cooled, at which point **1** forms a solid crystalline mass (from which crystals of **1**, for structural analysis, were extracted) that is difficult to further process. In contrast to this, it was easier to run this reaction in solvent (toluene) such that stirring could be maintained for the duration of the reaction and also the product formed as a granular powder that was preferable to handle for future processes, although the reaction did take longer with the use of solvent than without. The only advantage, for this present study, in preparing **1** without solvent was that crystals suitable for X-ray crystallographic analysis could be broken off from the resultant solid mass.

The traditional synthesis of a bis(indolenine)squaraine requires the use of a catalytic amount of quinoline in the reaction mixture. The products are usually collected following precipitation from the cooled solvent mixture. Preliminary attempts to prepare the *N*-propan-3-sulfonic acid derivative of a bis(indolenine)squaraine

yielded reaction mixtures with no precipitate, even upon concentration of the solvent mixture. Fortuitously, when the amount of quinoline in the reaction was increased to match the molar equivalent of the indolenine component (shown schematically in Fig. 1) then bright green crystals of **2a** precipitated and could be collected, washed and used without further purification, similar to *N*-alkyl derivatives of bis(indolenine)squaraine. Furthermore, **2a** was subsequently found to be highly water soluble. Crystals of **2a** were extracted directly from the reaction mixture, were recrystallized from chloroform and were analysed using X-ray crystallographic techniques.

Following the success of the synthesis of **2a**, a further twenty organic bases[2] were examined as catalysts in the reaction, although of those only three yielded crystals, from chloroform solution, suitable for structure determination. Three of the four (**2a**, **2b**, and **2d**) required synchrotron radiation due to the (lack of) size of the resultant crystals. These three involved the use of 5-nitroquinoline, 8-hydroxyquinoline and acridine, and their corresponding squaraine dyes (as per their crystal structures) are shown in Fig. 2. Of all the complexes prepared, only the four whose crystal structures could be determined are discussed in this study because they can provide the highest level of accuracy with respect to exact chemical composition, although particular molar absorptivity data from the other complexes is stated, where relevant and the squaraine derivative based on piperidine **2e** (shown in Fig. 3) is included because of its improved performance as a gel stain (in comparison to all twenty-one derivatives).

3.2. X-ray crystallographic analysis

The structure of **1** is shown in Fig. 4 and unsurprisingly, with three strong hydrogen bond acceptor atoms on the sulfonate group, there are two water molecules per sulfonate group, which add hydrogen bond donor atoms to the lattice. The concept of balancing the number of hydrogen-bond acceptor atoms by the addition of hydrogen-bond donor atoms is highlighted in reference [38]. All three sulfonate oxygen atoms are bound by hydrogen-bonding associations, one from O1W [O1W···O1 2.836(9) Å] and two from O2W [O2W···O2 2.847(10) Å and O2W···O3 2.876(10) Å (x, ½ − y, ½ + z)]. The second hydrogen atom on O1W hydrogen bonds to O2W [2.765(10) Å (−x, ½ + y, ½ − z)] and C—H···O close contacts from C4 to O1W [3.393(12) Å (x + 1, ½ − y, z − ½)], C5 to O1 [3.386(12) Å (x + 1, y, z)] and C11 to O1 [3.493(11) Å (−x, −y, −z)] also exist. The indolenine rings are off-set stacked, with minimal overlap, in pairs; interplanar distance >3.5 Å. The two latter C—H···O close contacts to O2 arise from C—H groups in an adjacent stacked pair.

The structure of **2a** is shown in Fig. 5 and similar to almost all of the bis(indolenine)squaraine crystal structures, the molecule is symmetrical with only half being in the asymmetric unit and the other half being generated across a centre of inversion. The squaraine moiety is essentially flat with the dihedral angle between the central 4-membered ring and the indolenine benzene ring being 16.4(4)°. The presence of the quinolinium cations seemingly prevents any charge-transfer stacking of the squaraine moieties. The squaraines do off-set stack, with no observable overlap, with interplanar distances >4 Å. In terms of other interactions, the only

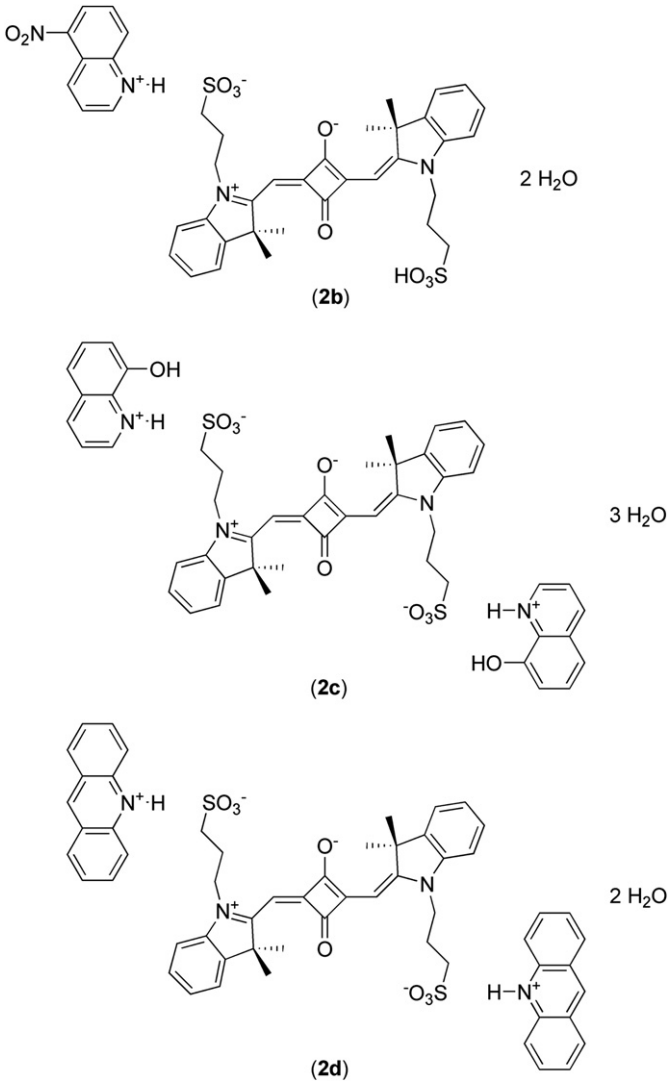

Fig. 2. Schematic illustrations of **2b**, **2c**, and **2d**, as determined by their crystal structures.

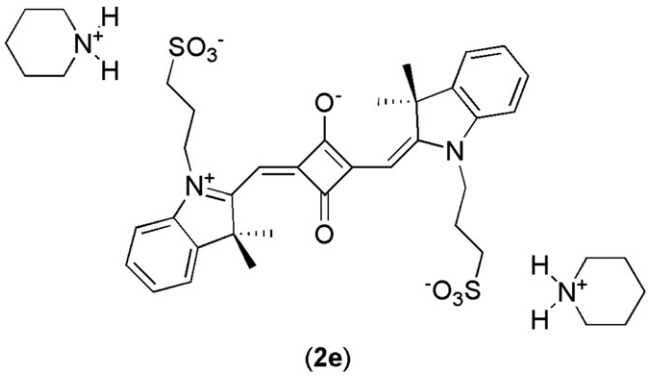

Fig. 3. Schematic illustration of the proposed structure of **2e**. An broad single unassigned peak in the ^{1}H NMR of **2e** at $\delta = 3.02$ ppm, coupled with the presence of a weak peak between 1640 and 1615 cm^{-1} and a possible strong O—H bending peak between 1410 and 1260 cm^{-1} in the infrared spectrum all suggest that **2e** contains waters of crystallization. $[2(C_5H_{12}N)^+(C_{32}H_{34}N_2O_8S_2)^{2-}\cdot{}^1/_2H_2O]$ (EA) (% found/calc.): C, 61.46/61.55; H, 7.14/7.19; N, 6.01/6.84.

[2] Quinaldine, lepidine, 5-nitroquinoline, 5-nitroisoquinoline, 6-methoxyquinoline, 8-hydroxyquinoline, acridine, 1,4-diaminocyclohexane, triethylamine, 4,4-dipyridine, morpholine, piperidine, 3-hydroxypyridine, 2-methyl-1,3-benzoxazole, 2-amino-1,3-thiazole, 2-amino-5-nitro-1,3-thiazole, 2-aminobenzo-1,3-thiazole, 2-amino-6-nitrobenzothiazole, 2-amino-1,3-thiazoline, 2-aminopyridine, and 2-amino-3-nitropyridine.

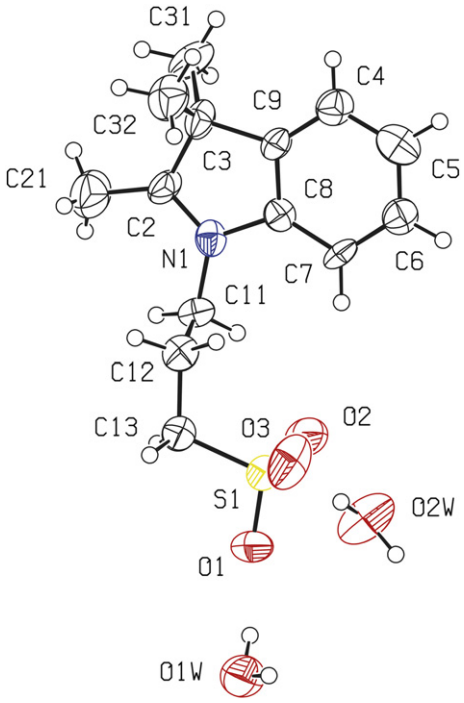

Fig. 4. ORTEP and atom naming scheme for **1** (displacement ellipsoids are drawn at 50% probability levels).

notable hydrogen-bonding association is between the quinolinium nitrogen atom and one of the sulfonate oxygen atoms [N2···O2 2.695(3) Å]. C—H···O close contacts exist to all sulfonate oxygen atoms but the only one worthy of note is that next to the N2—H···O association, which links C17 to O3 [3.220(3) Å and H17···O3 2.508(3) Å]. In the ^{1}H NMR spectrum for this compound the doublet expected for the quinolinium hydrogen atom (N^+H) could not be unambiguously identified so all similar peaks across the aromatic region were designated as aromatic hydrogen atoms (i.e. ArH).

The structure of **2b** surprisingly contains only one nitroquinolinium cation with the entire squaraine moiety being in the asymmetric unit. Although the sulfonic acid hydrogen atom could

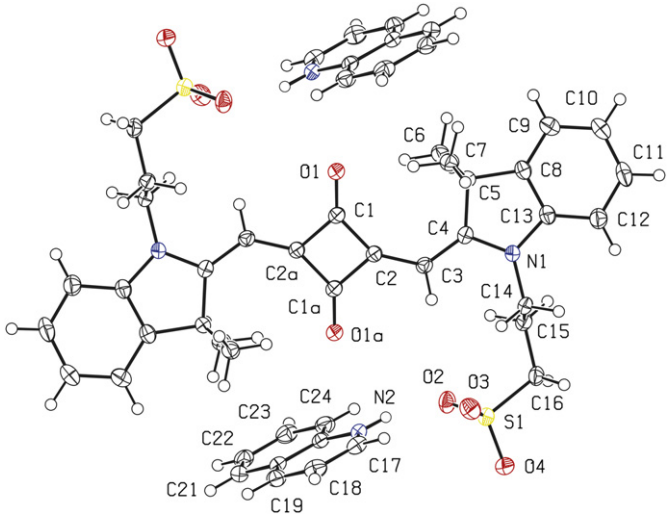

Fig. 5. ORTEP and atom naming scheme for **2a** (a = 1 − *x*, −*y*, 1 − *z*) (displacement ellipsoids are drawn at 50% probability levels) (atoms C20 and C25 are not named for image clarity).

not be located, on *Fourier* syntheses in the refinement, it is suspected to reside on O4 (hence being included at a generated position on that atom) because the other two sulfonic acid oxygen atoms are surrounded by hydrogen bond donor atoms and C—H···O close contacts plus O4, with an attached hydrogen atom, creates a long hydrogen bond to an adjacent indolenine nitrogen atom [O4···N1 3.371(6) Å, H···N 2.64(2) Å (*x*, 1 + *y*, *z*)]. The presence of a sulfonic acid group can be detected in the infrared spectrum of **2b** with characteristic C—SO_3H peaks at 1200 cm^{-1} and 1050 cm^{-1}. The nitroquinolinium in the structure is disordered equally across two sites, as is the sulfonate group that it associates with. The nature of the disorder is illustrated in Fig. 6, which contains two images, one of each disordered state. The basic difference between the two states is that in one the nitroquinolinium hydrogen bonds directly to a partial occupancy sulfonate oxygen atom [N5···O7 2.673(9) Å] whereas in the other state the cation associates to a half-occupancy water molecule [N3···O3W 2.602(6) Å], which in turn associates to different partial occupancy sulfonate oxygen atoms [O3W···O7A 2.683(6) Å, O3W···O7B 2.779(6) Å] as well as an adjacent sulfonic acid oxygen atom [O3W···O3 2.754(6) Å (*x*, −*y* + 2, *z* − ½)]. However, the disorder across the sulfonate group is more complex than illustrated in the two images of Fig. 6. The absence of a second cation subsequently leaves room for two water molecules (one being half occupancy) that hydrogen bond to each other [O2W···O1W 2.886(4) Å] in addition to the two remaining sulfonic acid oxygen atoms [O1W···O3 2.966(5) Å, O1W···O5 2.793(4) Å (*x*, *y* − 1, *z*)]. The squaraine moiety in this structure is essentially flat with dihedral angles between the two indolenine rings being 9.8(2)° and the angles between the two rings and the central 4-membered ring being 14.7(2)° and 5.3(2)°. The squaraine moieties arrange in off-set slip-stacked columns with interplanar distances >4.7 Å. The absence of the second cation indicates that these molecules may form first as the sulfonic acids that then protonate the available organic bases, precipitating out of the cooling solution as organic salts. For reasons currently unknown, this complex precipitated out of solution in a stable mono-cationic form having protonated only one base molecule per squaraine. It should be noted that this off-set in expected stoichiometry was not immediately obvious in any other form of chemical analysis performed on this complex, although careful examination of the ^{1}H NMR spectrum did suggest that only one cation was present. The disorder associated with the cation can also be detected in the 1H NMR through the splitting of two Ar-H doublet peaks, into two separate doublets each integrated at ½H. The split doublets at $\delta = 7.83$ ppm and 7.84 ppm most likely correspond to the hydrogen atoms of C36 and C45 whereas the split doublets at $\delta = 7.97$ and 7.99 ppm most likely belong to the hydrogen atoms of C33 and C43. The other peaks associated with the hydrogen atoms of the cation, except for the dd at $\delta = 9.10$ ppm, show signs of splitting into two equal parts, but not enough to be separately characterised. The presence of water in the structure had little effect on the ^{1}H NMR spectrum although a broad singlet peak at $\delta = 6.50$ ppm could account for a combination of the hydrogen atoms in each of the water molecules, the sulfonic acid group, plus the quinolinium hydrogen atom (i.e. $H_2O/SO_3H/N^+H$).

The structure of **2c** is illustrated in Fig. 7 and shows a full squaraine moiety in the asymmetric unit, along with two hydroxyquinolinium cations and three water molecules. The presence of these three water molecules (per asymmetric unit) gave rise to problems in the ^{1}H NMR with a broad water peak masking the expected NCH_2 peak around $\delta = 4.5$ ppm, as well as the hydroxyl hydrogen atom that was also expected in the same region. In the crystal structure, the squaraine moieties are essentially planar with dihedral angles between the two indolenine rings being 1.6(2)° and then between the two outer rings and the central 4-membered ring

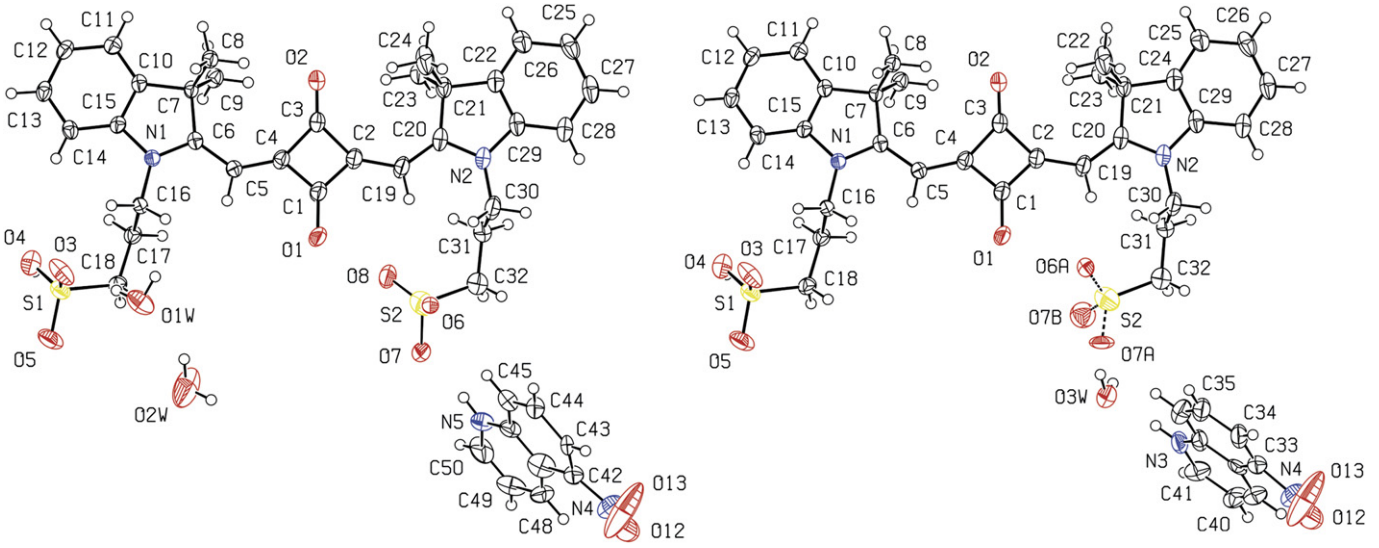

Fig. 6. ORTEP and atom naming scheme for **2b**, showing the two separate disordered forms (displacement ellipsoids are drawn at 50% probability levels) (atoms C36–C39, C46, C47 are not named for image clarity).

being 7.5(2)° and 8.2(2)°. The squaraines are also slip-stacked in columns with interplanar distances >4.6 Å. One possible reason for the asymmetry in this structure may arise in the difference in association that the two hydroxyquinoliniums make with their respective sulfonate groups. One of the cations hydrogen bonds (through the N^+–H donor) directly with a sulfonate oxygen atom [N3···O3 2.813(4) Å ($-x+1, -y, -z$)] whereas the other hydrogen bonds (through the N^+–H donor) to one of the water molecules [N4···O3W 2.599(5) Å]. O3W in turn hydrogen bonds to O7 and O2W [2.695(4) Å ($-x+1, -y+1, -z$) and 2.711(4) Å ($-x+2, -y, -z+1$) respectively]. Both O2W and O1W form hydrogen-bonded rings across separate inversion centres each linking with two separate oxygen atoms from adjacent sulfonate groups [O2W···O5 2.740(4) Å and O2W···O4 2.796(4) Å ($-x+2, -y, -z+1$); O1W···O8 2.752(4) Å and O1W···O6 2.835(5) Å ($-x, -y+1, -z-1$)]. All sulfonate oxygen atoms are bound by strong hydrogen-bonding associations. The two hydroxyl groups separately hydrogen bond to the two squarate oxygen atoms [O9···O2 2.577(4) Å and O10···O1 2.590(4) Å]. The positioning of the 8-hydroxyquinoline groups in this structure may also give rise to ring current effects, thus creating the lack of resolution observed across the aromatic hydrogen atom region in the ^{1}H NMR for this molecule. The low calibre of this structure is due to poor crystal quality, which runs parallel to the poor quality of the ^{1}H NMR spectrum.

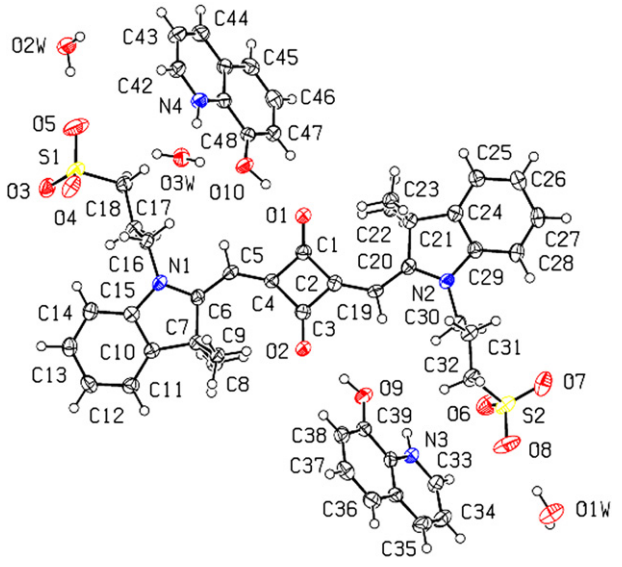

Fig. 7. ORTEP and atom naming scheme for **2c** (displacement ellipsoids are drawn at 50% probability levels) (atoms C40, C41, C49 and C50 are not named for image clarity).

The structure of **2d** is illustrated in Fig. 8 and, similar to **2c**, shows an essentially flat squaraine moiety that packs in slip-stacked columns with interplanar distances the same as the previous structure. However, unlike **2c**, **2d** is symmetrical, residing across an inversion centre; the dihedral angle between the indolenine ring and the central 4-membered ring is 5.5(2)°. Similar to **2a**, in this structure the acridinium cation associates directly with a sulfonate oxygen atom [N2···O2 2.670(8) Å]. The one water molecule in the asymmetric unit hydrogen bonds to both O2 and O4, which are from separate sulfonate groups [O1W···O2 2.846(9) Å and O1W···O4 2.805(9) Å ($1+x, y, z$)]. There are also two similar bifurcated C–H···O close contacts worthy of note because one is the only close contact with sulfanate oxygen atom O3 [C18···O3 3.064(9) Å, H···O 2.462(9) Å ($x, 1+y, z$) and C19···O3 3.174(9) Å, H···O 2.694(9) Å ($x, 1+y, z$)] while the other slots into the back of the water molecule [C21···O1W 3.122(9) Å, H···O 2.219(9) Å ($3-x, 3-y, 1-z$) and C22···O1W 3.469(9) Å, H···O 2.699(9) Å ($3-x, 3-y, 1-z$)]. Both close contact associations each involve two adjacent hydrogen atoms from an acridinium ring. The low calibre of this structure is due to poor crystal quality.

3.3. Molar absorptivity

Examination of the molar absorptivity for **2a**–**2d**, in water, shows that the presence of different cations can affect the colour intensity of the squaraine dye. Of the four, **2b** has the highest molar absorptivity although this may be due to the fact that there is only one cation per squaraine unit in this complex, whereas the other three each have two. Of the other three, there is a significant drop (approximately by half) from **2a** and **2c** to **2d** (the acridinium complex). If all twenty-one complexes are considered then the range of molar absorptivities extends from 308,823 L mol^{-1} cm^{-1}

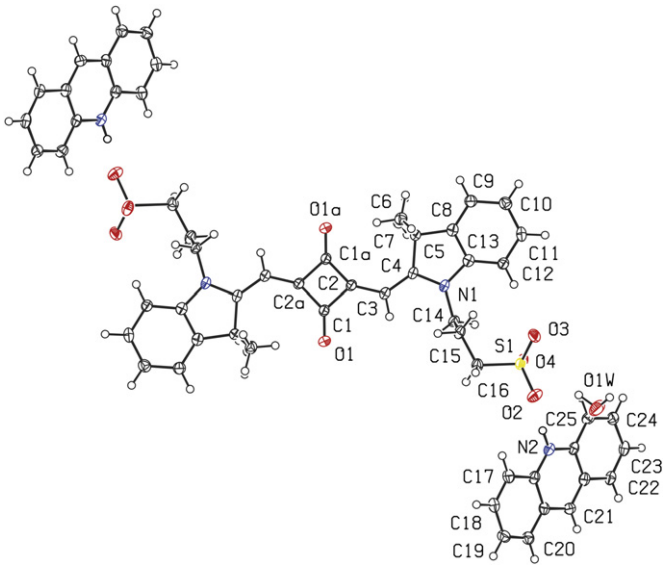

Fig. 8. ORTEP and atom naming scheme for **2d** (a = $-x$, $2-y$, $-z$) (displacement ellipsoids are drawn at 50% probability levels) (atoms C26–C29 are not named for image clarity).

(for the 2-amino-1,3-thiazolium complex) to 132,127 L mol^{-1} cm^{-1} (for the 2-amino-5-nitro-1,3-thiazolium complex). Interestingly, for all complexes, irrespective of the cation, the absorption maximum (λ_{max}) remained unchanged at 624–625 nm, including **2b**, which was the only one of the series to differ in precipitate colour. However, for the purposes of examining these types of dyes as colorimetric stains for SDS-PAGE, it was decided that only **2a** and **2c** were to be further examined because **2b** was not representative of the other three (and most likely not representative of any of the other dyes whose crystal structures could not be determined), and **2d** lacked colorimetric intensity, having a molar absorptivity of approximately half that of **2a** and **2c**. **2d** also lacked the solubility in water to create solutions of concentrations higher than 1×10^{-5} M.

3.4. Colorimetric staining using *2a*

After fixing in an aqueous solution containing 10% methanol and 10% acetic acid, and rinsing twice in deionised water for 10 min, the prepared gels (loaded with a BSA standard and lysed mitochondrial supernatant) were stained in aqueous solutions of **2a**, with concentrations ranging from 1×10^{-2} to -1×10^{-5} M for 1 h, followed by destaining in water. It was observed that the gels stained in dye solution concentrations below 1×10^{-3} M had noticeably lower stain intensity than those stained in the higher concentrations. Stain solutions with concentrations above 1×10^{-3} M did not show any increase in stain intensity, but did take much longer to destain, thus a concentration of 1×10^{-3} M was determined as the optimum stain solution concentration for **2a**. Gels stained at this concentration gave a pattern that closely resembled that of a duplicate gel stained with CBB. In terms of residual background coloration, all of the gels stained using **2a** in water retained a very pale blue background. However, a 4–5 h destain period and using 100 mL destain volume, with replacing the water every 30 min, gave a pale background coloration that was much lower than the typically patchy, purple background of a CBB stained gel. It was possible, using 100 mL destain volume, to achieve a completely clear background with **2a**, but this took several days and countless changes of destain water, and led to a significant loss of stain intensity on the protein bands. Similarly, gels stained with CBB could also produce an almost clear background after several days, and countless changes of destain solution.

In terms of decreasing the background coloration, **2a** stained gels were destained using 100 mL of an aqueous solution containing 10% methanol and 10% acetic acid (the standard CBB destain solution), which resulted in a reduced destain period of 3 h and yielded a suitably clear background. The intensity of the stained bands was reduced compared to the gels destained using water, but all of the bands were still present on the gels, and the pattern was still comparable to that of duplicate gels stained with CBB. However, variation of the water destain volume for **2a** stained gels showed that although greater volumes decreased the time taken to achieve a suitable background, with a 200 mL volume reducing the destain period to 2 h, compared to the minimum volume required to cover the gel (25 mL) taking 4 h, comparison of the protein patterns showed that the greater volumes also decreased the stain intensity, with complete loss of stain intensity from some of the lower concentration protein bands. The minimum destain volume (25 mL) produced by far the best quality stains, with the most bands and the greatest depth of stain. These gels were superior to the CBB stained gels in respect of resolution of the bands and contrast, due to the strong CBB background.

The amount of time allowed between changing the destain solution was also investigated, showing that the destain rate could be increased by changing the solution more frequently, although this resulted in a reduction in the intensity of the stain on the protein bands. Changing the solutions every 15 min produced gels with suitably clear backgrounds in 1.5 h. However, changing the solution when it appeared to have reached equilibrium with the gel background (i.e. being of the same dye intensity in both stain solution and gel) took 4 h to produce a suitably clear background, but resulted in the greatest intensity of stain on the protein bands and the lowest limit of detection (LOD).

Comparison of gels loaded with both the 'homemade' protein ladder and lysed mitochondrial supernatant proteins, stained with **2a**, with those stained with non-colloidal CBB, showed that both dyes achieve quantitatively and qualitatively approximately the same results. In addition, **2a** produces a suitably clear background and (in comparison to CBB) displays greater resolution of the tightly stacked protein bands. It should be noted that comments on the performance of CBB in this study are made from results that were obtained experimentally during this study, staining gels in parallel with the squaraine dyes. The authors acknowledge that other forms of CBB are commercially available that display significantly better performance parameters than that of the form of CBB employed. However, for this study it was decided that the performance of the squaraine dyes should be compared against the CBB used, purely because it is the most common, readily available form of CBB whose performance can be related directly with the original publication [34].

3.5. Colorimetric staining using *2c*

SDS-PAGE gels stained with solutions of **2c** produced patterns that were qualitatively identical to those produced for **2a** and CBB, but the stain coloration was of a lower intensity. Increasing the concentration of **2c** above 1×10^{-3} M in the stain solution, to try and increase the stain intensity, resulted in **2c** precipitating within the gel matrix, causing a speckled background. Increasing the stain time to 2 h resulted in greater stain intensity without the speckled background stain. However, this did not increase the destain time, which remained at 5 h irrespective of the staining time. Comparison with duplicate gels stained with CBB showed similar advantages to **2a** with better resolution of closely stacked bands and a suitably clear background, although destaining took a little longer.

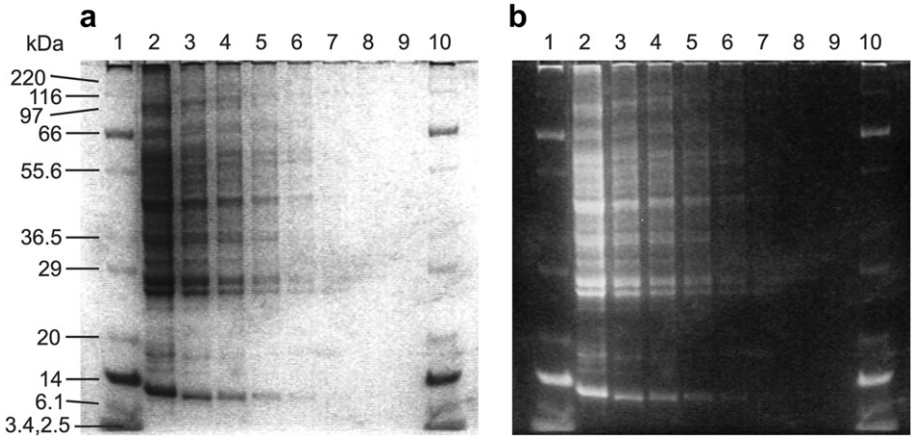

Fig. 9. SDS-PAGE gels loaded with ProteMix protein standard (Lanes 1 and 10), and a two-fold serial dilution of lysed (rat liver) mitochondrial supernatant from 12 μg of total protein (Lanes 2–9), stained with a 1×10^{-3} M aqueous solution of **2e** and imaged using a Bio-Rad gel documentation system, with a white light epi-illuminator and a white background (a) and in UV excitation/fluorescent imaging mode (b).

3.6. Colorimetric staining using *2e*

Of the remaining organic cations listed in footnote,[1] the squaraine dye prepared using piperidine as a catalyst (**2e**) (Fig. 3) was judged to be the best colorimetric stain overall, not only because performance included a marginally clearer resolution of the closely stacked lysed mitochondrial supernatant proteins (Fig. 9a), aided by a clear background, but mainly because **2e** exhibited an increased destaining time, as little as 2.5 h to produce a gel ready for imaging. The dynamic linear range of this stain was estimated, using densitometry calculations on the Bio-Rad gel documentation system (using Quantity One software), on the gel images and showed a colorimetric linear range of 10–100 μg/mL of BSA. Finally, the stained gels were stable for several hours, in either water or the CBB destain solution, before the diffusion of the dye reduced the quality of the images. An additional factor in the use of **2e** is that if an image of a gel is recorded in the UV excitation/fluorescent imaging mode (on the Bio-Rad gel documentation system), with a UV excitation filter (Schott UG 11 filter) underneath the gel and a long pass or edge type filter, which sharply cuts light below 630 nm and a minimum of 50% transmittance 645–2750 nm (Oriel LP63 filter), covering the camera, then it is possible to record a fluorescent image of the gel (Fig. 9b). Unfortunately, in this case gel imaging using fluorescence does not increase the LOD, as it would normally be expected to, although for some bands visualization can be improved.

3.7. Reuse of the stain solution

During this investigation it was observed that non-colloidal, CBB stain solutions were reusable at least 10 times, provided that the proteins were fixed prior to staining. Because the non-colloidal CBB stain solutions contained a significant amount of methanol and acetic acid, the stain solution would fix, as well as stain the proteins in the gels, but only doing this reduced the number of times the stain solution could be reused to 5–6 times, due to the build-up of SDS concentration in the stain solution, thus preventing the dye from binding to the proteins. Staining SDS-PAGE mini gels with **2e** reduced the concentration of the dye in the solution by 20–25%, determined using visible spectroscopy against a serial dilution of known **2e** standards. Reusing the stain solution resulted in significantly less colorimetric stain intensity, which could be improved a little by increasing the stain time to 2 or more hours. Even when left to stain overnight the intensity was never as great as it had been with the first use. Further reuse of the stain solution consistently produced unsatisfactory results. However, it was found that by adding fresh dye to the stain solution, to restore it to its original concentration, the stain solution could then be reused almost endlessly (if the gels were fixed prior to staining).

4. Conclusions

In this study we have shown that the difficulties encountered in the synthesis of a dual-pendant sulfonate bis(indolenine)squaraine dye can be overcome through the use of equimolar amounts of the common reaction catalyst, thus creating an organic salt between the sulfonate groups and the protonated catalyst. We have also shown that a range of water-soluble dyes can be prepared, by changing the catalyst. Crystal structures of four subsequent derivatives, prepared in this manner, have shown that, although the squaraine moieties remain essentially planar, the packing lattices can vary significantly, and the expectation that both sulfonic acid groups will protonate a stoichiometric amount of the available organic base catalyst is also shown by one structure to not be fully true. Two of the dyes prepared, crystal structure determined, plus an additional dye (structure unknown) proved to be suitable as colorimetric stains for protein separation in SDS-PAGE, and an optimal method for staining was determined. In all cases the results were compared against non-colloidal CBB and it was found that the LOD for all squaraine derivatives examined was similar to CBB, although the resolution between protein bands was improved and gels stained with the one of the dyes could be imaged in UV excitation/fluorescent imaging mode. The image robustness (or colour fastness) of all squaraines was found to be good for only a few hours.

Disclosure statement

This work was initially disclosed under a GB patent filing 'Fluorescent Protein Detector' (No. GB 0323171.9) on the 3rd October 2003; PCT 30th September 2004; ceased March 2008.

Acknowledgements

The authors wish to thank the Faculty of Health and Life Sciences for financial assistance and thank the EPSRC National Crystallography Service (Southampton University, England) and Synchrotron Service (Newcastle University, England), John Langley (Southampton University, England) for the collection of electrospray mass spectroscopy, and Darren Hamilton (Mt Hollyoke

College, USA) for the collection of ^{1}H NMR data. Medac Limited (UK) is thanked for C,H,N analysis. AK acknowledges funding from an EPSRC industrial case award sponsored by Scie-Plas Limited, Biochrom Limited and Hoefer Inc. Angela Miller is thanked for running a preliminary gel to prove the concept that these dual pendant squaraines could colorimetrically stain proteins in this form. Steve Marriott (Biochrom Limited) is thanked for his technical assistance.

References

[1] Sprenger H-E, Ziegenbein W. The cyclobutenediylium cation, a novel chromophore from squaric acid. Angew Chem Int Ed 1967;6:553–4.
[2] Schmidt AH. Reaktionen von quadratsäure und quadratsäure-derivaten. Synthesis 1980;12:961–94.
[3] McEwen JJ, Wallace KJ. Squaraine dyes in molecular recognition and self-assembly. Chem Commun; 2009:6339–51.
[4] Kuramoto N, Natsukawa K, Asao K. Synthesis and characterisation of deep-coloured squarylium dyes for laser optical recording media. Dyes Pigm 1989;11:21–35.
[5] Zhang B, Zhao W, Cao Y, Wang X, Zhang Z, Jiang X, et al. Photoluminescence and electroluminescence of squarylium cyanine dyes. Synth Met 1997;91:237–41.
[6] Dilek G, Akkaya EU. Novel squaraine signalling Zn(II) ions: three-state fluorescence response to a single input. Tetrahedron Lett 2000;41:3721–4.
[7] Meadows F, Narayanan N, Patonay G. Determination of protein-dye association by near infrared fluorescence-detected circular dichroism. Talanta 2000; 50:1149–55.
[8] Scherer D, Dörfler R, Feldner A, Vogtmann T, Schwoerer M, Lawrentz U, et al. Two-photon states in squaraine monomers and oligomers. Chem Phys 2002; 279:179–207.
[9] Jiao G-S, Loudet A, Lee HB, Kalinin S, Johansson LB-Å. Syntheses and spectroscopic properties of energy transfer systems based on squaraines. Tetrahedron 2003;59:3109–16.
[10] He Y, Zhou W, Wu F, Li M, Wang E. Photoreaction and photopolymerization studies on squaraine dyes/iodonium salts combination. J Photochem Photobio A Chem 2004;162:463–71.
[11] Grytsenko KP, Schrader S. Nanoclusters in polymer matrices prepared by co-deposition from a gas phase. Adv Colloid Interface Sci 2005;116:263–76.
[12] Kawabata Y, Sekiguchi T, Tanaka M, Nakamura T, Komizu H, Honda K, et al. Supermolecular structure in the Langmuir-Blodgett films of a surface-active dye-fatty acid mixed system. J Am Chem Soc 1985;107:5270–1.
[13] Matsumoto M, Nakamura T, Tanaka M, Sekiguchi T, Komizu H, Matsuzaki SY, et al. Structure study of supermolecular layers in Langmuir-Blodgett films. Surface active squarylium dye-fatty acid binary mixed system. Bull Chem Soc Jpn 1987;60:2737–42.
[14] Mathis KS, Kuzyk MG, Dirk CW, Tan A, Martinez S, Gampos G. Mechanisms of the nonlinear optical properties of squaraine dyes in poly(methyl methacrylate) polymer. J Opt Soc Am B 1998;15:871–83.
[15] Tong L, Bi-Xian P, Fenglian B. The structure and ^{13}C-NMR of an indolenium squaraine dye. Dyes Pigm 1999;43:67–71.
[16] Lawrentz U, Grahn W, Dix I, Jones PG. 2,4-Bis{[6-(2,2-dimethylpropyl)-3-ethyl-1,3-benzothiazol-2(3H)-ylidene]methyl}cyclobutenediylium-1,3-diolate. Acta Cryst 2001;C57:126–8.
[17] Lynch DE. 2,4-Bis(3,3-dimethyl-1-octylindolin-2-ylidenemethyl)cyclobutenediylio-1,3-diolate. Acta Cryst 2002;E58:o1025–7.
[18] Dimitriev OP. Anomalous aggregation of squaraine dyes in confined solutions. J Mol Liquids 2005;120:131–3.
[19] Terpetschnig E, Szmacinski H, Lakowicz JR. Synthesis, spectral properties and photostabilities of symmetrical and unsymmetrical squaraines; a new class of fluorophores with long-wavelength excitation and emission. Anal Chim Acta 1993;282:633–41.
[20] Terpetschnig E, Lakowicz JR. Synthesis and characterisation of unsymmetrical squaraines: a new class of cyanine dyes. Dyes Pigm 1993;21:227–34.
[21] Terpetschnig E, Szmacinski H, Ozinskas A, Lakowicz JR. Synthesis of squaraine-N-hydroxysuccinamide esters and their biological application as long-wavelength fluorescent labels. Anal Biochem 1993;217:197–204.
[22] Mank AJG, van der Laan HTC, Lingeman H, Gooijer C, Brinkman UATh, Velthorst NH. Visible diode laser-induced fluorescence detection in liquid chromatography after precolumn derivatization of amines. Anal Chem 1995; 67:1742–8.
[23] Kukrer B, Akkaya EU. Red to IR fluorescent signalling of carbohydrates. Tetrahedron Lett 1999;40:9125–8.
[24] Oswald B, Patsenker L, Duschl J, Szmacinski H, Wolfbeis OS, Terpetschnig E. Synthesis, spectral properties, and detection limits of reactive squaraine dyes, a new class of diode laser compatible fluorescent protein labels. Bioconjug Chem 1999;10:925–31.
[25] Oswald B, Lehmann F, Simon L, Terpetschnig E, Wolfbeis O. Red laser-induced fluorescence energy transfer in an immunosystem. Anal Biochem 2000;280: 272–7.
[26] Nizomov N, Ismailov ZF, Nizamov SN, Salakhitdinova MK, Tatarets AL, Patsenker LD, et al. Spectral-luminescent study of interaction of squaraine dyes with biological substances. J Mol Struct 2006;788:36–42.
[27] Tatarets AL, Fedyunyayeva IA, Dyubko TS, Povrozin YA, Doroshenko AO, Terpetschnig EA, et al. Synthesis of water-soluble, ring-substituted squaraine dyes and their evaluation as fluorescent probes and labels. Anal Chim Acta 2006;570:214–23.
[28] Volkova KD, Kovalska VB, Tatarets AL, Patsenker LD, Kryvorotenko DV, Yarmoluk SM. Spectroscopic study of squaraines as protein-sensitive fluorescent dyes. Dyes Pigm 2007;72:285–92.
[29] Hamilton AL, West RM, Cummins WJ, Briggs MSJ, Bruce IE. Squaraine dyes and their use in fluorescent sequencing method. Patent 1997:US 6,140,494.
[30] Singh R, Gorski G, Frenzel G. Bridged fluorescent dyes, their preparation and their use in assays. Patent 2000:US 6,403,807.
[31] West RM, Cummins WJ, Nairne RJD, Bull MG. Squaraine dyes. Patent 2000:WO 00/58405.
[32] Deroover G, Missfeldt M, Simon L. Use of acylsulfonamido-substituted polymethine dyes as fluorescence dyes and/or markers. Patent 2001:US 6,995,262.
[33] Weaver GW, Smith A, Palmer DA, French MT. Long wavelength 4-[1-(naphtha[1,2-d]thiazol-1-ium-2-yl)methylidene]-3-oxo-2-[(2,3-dihydro-1H-indol-2-yliden)methyl]cyclobuten-1-olate based fluorescent dyes. Patent 2001:GB 2,373,509.
[34] Laemmli UK. Cleavage of structural proteins during the assembly of the head of bacteriophage T4. Nature 1970;227:680–5.
[35] Suzuki Y, Yokoyama K. A protein-responsive chromophore based on squaraine and its application to visual protein detectionon a gel for SDS-PAGE. Angew Chem Int Ed 2007;46:4097–9.
[36] Lowry OH, Rosebrough NJ, Farr AL, Randall RJ. Protein measurement with the folin phenol reagent. J Biol Chem 1951;193:265–75.
[37] Havinga EE, Pomp A, Ten Hoeve W, Wynberg H. Water-soluble polysquaraines and polycroconaines. Synth Met 1995;69:581–2.
[38] Desiraju GR. Hydration in organic crystals: prediction from molecular structure. J Chem Soc Chem Commun; 1991:426–8.